Technical University of Denmark

DTU

Extreme wind atlas from the selective dynamical downscaling method

Larsén, Xiaoli Guo; Badger, Jake; Hahmann, Andrea N.; Ott, Søren

[Link back to DTU Orbit](#)

DTU Library
Technical Information Center of Denmark

Extreme wind atlas from the selective dynamical downscaling method

X.G. Larsén, J. Badger, A. Hahmann and S. Ott

xgal@risoe.dtu.dk

Wind Energy Division

Risø National Laboratory for Sustainable Energy

Technical University of Denmark

4000 Roskilde, Denmark

Abstract

We developed a dynamical downscaling method to obtain the extreme wind atlas using simulations of the selected strongest storms by Weather Research and Forecasting (WRF) model. This method consists of three steps, namely, identification of storms, WRF simulation and post-processing. The output will be atlases for generalized extreme winds, namely over a homogeneous surface with a certain roughness, e.g. 0.05 m, at a certain height, e.g. 10 m. This provides platforms for data validation and for passing the mesoscale extreme winds to specific places through microscale modeling. The results are compared to measurements and they are promising.

Keywords: Extreme wind atlas, WRF, selective dynamical downscaling, post-processing

1 Introduction

A reliable estimate of the extreme winds, often the 50-year wind, is important for wind turbine manufacturers and wind farm developers. For each wind turbine site the most likely extreme wind has to be estimated in order to make sure that winds will not exceed the turbine's design specification and avoid being unrealistically over-specified. Here, the extreme winds are 10 min values in accordance with the Eurocode[1].

The current study confronts the most common problem in estimating the extreme wind for a specific wind farm site, i.e. the shortage of long term observations of reliable quality. The global re-analysis data have shown to be useful in providing background forcing to microscale models in simulating the extreme winds in places where extreme wind events are of synoptical scale ([2]), mesoscale modeling is needed for places where extreme wind events inducing mesoscale meteorological phenomena. However, resolving extreme wind events is not an easy task for regional climate modeling, especially in a climatological context ([3, 4]).

A new method, called the "selective dynamical mesoscale modeling method", is developed using mesoscale modeling, in accordance with the Annual Maximum Method (AMM)(Section 2.2) for obtaining the 50-year wind and it is introduced in Section 2.1. This method has been applied to two cases, one for Denmark where the extreme winds are of synoptical phenomena and one for the Gulf of Suez where the mesoscale channeling winds contribute significantly to the extreme winds.

For site use, the mesoscale modeled winds can not be applied directly without taking into account the microscale orographic and roughness effects. Two approaches of post-processing to generalize modeled winds are hence introduced (Section 5, see also [5]). The generalization of the winds provides a platform for coupling the information from mesoscale modeling to microscale modeling. The generalization also aids in the comparison of the

measured and simulated winds, otherwise the uncertainty is large in the comparison of point measurements and spatially averaged simulated values.

The results are validated by measurements (Section 3) and presented in Section 6, followed by Discussions and Conclusions in Sections 7 and 8.

2   Method

2.1   The selective dynamical downscaling modeling method

When applying this selective dynamical downscaling modeling method, first, for a particular area, we use the surface and geostrophic wind calculated from NCEP/NCAR reanalysis data (horizontal resolution of $\sim 2.5°$ and 6 hourly) to identify the strongest yearly wind events for each and every grid point in this area. Figure 1 shows an example for the Denmark case. Thus a collection of storm episodes, here for the 20 grid points we get 58 storms for the period 1999 - 2010 are identified. Second, we use the NCEP final analysis data (horizontal resolution of $1°$, 6 hourly) to drive the mesoscale WRF (Weather Research and Forecasting) model to obtain the mesoscale wind fields, for all storm episodes. We use the $1°$ data to drive WRF instead of the reanalysis because they provide much better resolved storm structure at the beginning. Thus the spin-up time for the simulation is only a couple of hours. In addition, because the storms normally do not last more than a few days, we do not need the nudging technique to prevent the model from drifting during the storm life time. This, however, is a big issue when using coarse resolution data for the boundary conditions. Although FNL data are only available from 1999, they will grow with time. Third, for each and every one of the mesoscale grid points the annual wind maxima are found and put through the post-processing procedure and finally the values are used to calculate the 50-year wind. This method is efficient; we can easily run the model at very fine horizontal resolution such as 5 km and 3 km, which is a big challenge for most climate runs.
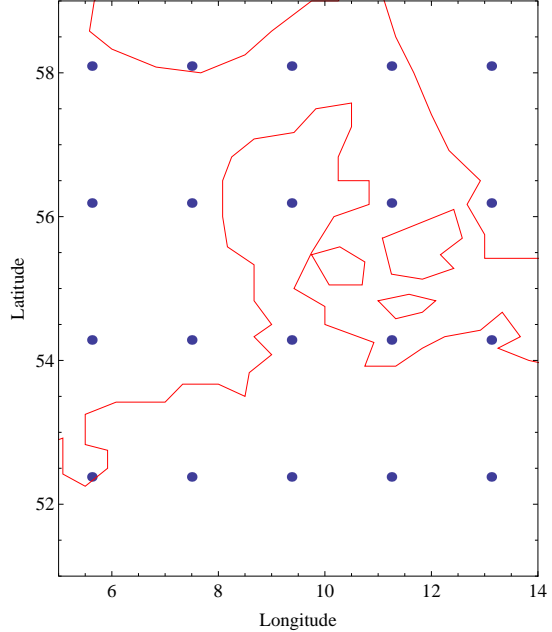

Figure 1: Grid points for the NCEP/NCAR reanalysis data where yearly wind maxima are identified.

2.2   The Annual Maximum Method

The Annual Maximum Method is used to calculate the 50-year wind. For the more detailed derivation, refer to e.g.[6, 2]. Briefly, the annual maximum winds from n years are first sorted in ascending order as U_i^{max}, where $i = 1, ..., n$. If the tail of the wind distribution is exponential, then the extreme winds have a double exponential accumulated probability $F(U)$:

$$F(U) = \exp(-\exp(-\alpha(U - \beta))) \qquad (1)$$

We use the Gumbel extreme wind distribution to fit the set of annual wind maxima. The coefficients α and β are obtained through the probability-weighted moment procedure:

$$\alpha = \frac{\ln 2}{2b_1 - \overline{U^{max}}}, \ \beta = \overline{U^{max}} - \frac{\gamma_E}{\alpha} \qquad (2)$$

where $\gamma_E \approx 0.577216$ is the Euler constant, $\overline{U^{max}}$ is the mean of U_i^{max} and b_1 is calculated from

$$b_1 = \frac{1}{n} \sum_{i=1}^{n} \frac{i-1}{n-1} U_i^{max} \qquad (3)$$

2

The relation between $F(U)$ and the reoccurrence interval T is

$$T = (1 - F(U_T))^{-1} \qquad (4)$$

Substituting Equation (1) into Equation (4) gives the T year wind speed

$$U_T = \alpha^{-1} \ln T + \beta \qquad (5)$$

[7] gave the estimation of uncertainty of U_T, which could be calculated from uncertainties on α and β:

$$\sigma(U_T) = \frac{\pi}{\alpha} \sqrt{\frac{1 + 1.14 k_T + 1.10 k_T^2}{6n}} \qquad (6)$$

with

$$k_T = \frac{\sqrt{6}}{\pi} (\ln T - \gamma_E) \qquad (7)$$

The uncertainty is estimated as the 95% confidence interval here and it is obtained by $1.96 \cdot \sigma(U_T)$.

3   Measurements

We use the measurements to validate 1) wind and other meteorological parameters variations during each storm at the grid points closest to the measurement sites; 2) the 50-year winds, with and without the post-processing. For the Denmark case, the measurements are from stations over Denmark and a few from Sweden and Germany, see details in Table 1 and the locations of the stations in Figure 2. Only data that are longer than 7 years with reliable quality are used for calculation of the 50-year wind.

4   The WRF model and the setup

The WRF Advanced research WRF (ARW) core version 3.1 is used for the mesoscale simulation. Together with the FNL data, the half-degree sea surface temperature from NCEP (ftp://polar.ncep/noaa.gov/pub/history/sst) is used. The Yonsei University Planetary Boundary Layer scheme is used, and for the microphysics, the Liu et al. scheme is chosen. The selection of
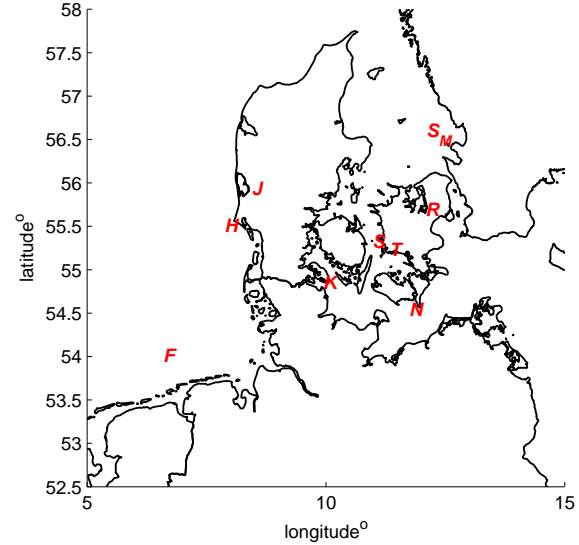

Figure 2: Map of Denmark and surroundings. The locations of the stations are marked by their initials, refer to Table 1.

the schemes are based on individual storm validation using measurements. Figure 3 shows three nested domains for the Denmark case, 37 vertical levels are used in all domains. The horizontal resolutions for the Denmark case are set as $45 - 15 - 5$ km (domain I-II-III) and for the Gulf of Suez case they are set as $27 - 9 - 3$ km. One-way nesting technique is used. The time step for domain-I is 4 minutes for the Denmark case and 2 minutes for the Gulf of Suez case, respectively. The output is recorded every 10 minutes. Given the characteristics of the extreme winds in the two areas, the extreme wind events do not last more than two days. The simulation is thus limited to a length of 2 days, no nudging is used.

5   The post-processing

Post-processing is applied both to measurements and simulated data. The purpose is to convert the winds, both simulated and measured, to standard conditions, namely to the same roughness length and same height, the so-called "standard wind", u_{st}. Thus, they could be reasonably compared. We call this process "generalization".

Table 1: Details of measurements for the Denmark case

Stations	Data Period	Height (m)	Initials as in Fig. 2
Sprogø	1979 - 1999	70	S
Tystofte	1982 - 2010	39	T
Kegnæs	1991 - 2006	23.4	K
Jylex	1983 - 2004	24	J
Risø	1991 - 2010	76.6	R
Horns Rev	1999 - 2006	62	H
Nysted	2004 - 2008	69	R
FINO1	2004 - 2010	50	F
S.Middelgrund	2008 - 2010	60	S_M

Figure 3: Three model domains shown as topography for domain I.

The correction for measurements are done with the WAsP cleaning procedure and the details can be found in [8, 6, 2]. In short, the speed-up effects due to orography and upstream roughness change are removed from the observed wind speed through the coefficients s_o (for orography) and s_r (for roughness change):

$$u_z = \frac{u_{0,z}}{(1 + s_o)(1 + s_r)} \tag{8}$$

where $u_{0,z}$ is the observed wind speed at a height z. The corresponding surface friction velocity u_* can then be calculated with u_z and area-averaged surface roughness length z_0 through the surface logarithmic law:

$$u_* = \frac{\kappa u_z}{\ln(z/z_0)} \tag{9}$$

where $\kappa = 0.4$ is the von Kármán constant. The core idea of the post-processing is that the large scale wind is the same over the two different surface conditions before and after the post-processing. This large scale wind here is the wind above the boundary layer, here the geostrophic wind G, can be calculated from u_* through the geostrophic drag law (e.g. [9]):

$$G = \frac{u_*}{\kappa} \sqrt{(\ln \frac{u_*}{f z_0} - A)^2 + B^2} \tag{10}$$

where f is the Coriolis parameter, $A = 1.8$ and $B = 4.5$ are dimensionless parameters ([10]). Neutral conditions are assumed, which is reasonable in extreme wind conditions. Under the same G but new roughness length, here $z_{0,r} = 0.05$ m, a new friction velocity, $u_{*,r}$, is obtained through
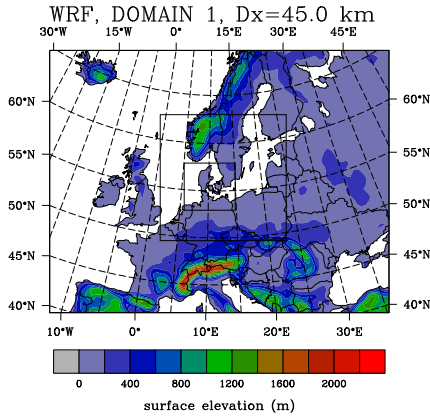
4

Equation (10). Using this new set of $u_{*,r}$ and $z_{0,r}$ and Equation (9), we obtain the standard wind u_{st}.

For the WRF simulated winds, two approaches are used.

5.1 Approach-I

Approach-I ignores the effects of orography and upstream roughness change and takes into account the local roughness effect. For each mesoscale grid point in domain III, there is a set of parameters u_z and z_0. From Equations (9) and (10), a u_{st} is derived, starting with Equations (9) through (10) and use Equation (9) again.

5.2 Approach-II

Approach-II differs from approach-I in that the directional roughness z_0 is used in Equation (9) and in that it takes into account of the effects of directional topographical and upstream roughness change. As explained in [5], the wind direction dependent upstream roughness is evaluated using the linear computational model (LINCOM), developed at Risø-DTU. The effective upstream roughnesses for a number of directional sectors are obtained. Here we use 12 sectors. LINCOM also gives, for all mesoscale model grid points, the perturbation to the wind speed given by orography (i.e. speed up at hills) and roughness change for 12 sectors. These perturbations can be expressed as generalization factors (see Figure 4 in [5]). The sector dependent effective roughness and the generalization factors form a look-up table for each mesoscale model grid point. For each of the storm episodes, the application of the generalization procedure is done through

- Equation (8), the generalization factors are applied to the simulated wind to give a corrected simulated wind,

- Equation (9) and Equation (10) are used to obtain the frictional velocity and the geostrophic wind using the effective roughness length and the corrected simulated wind,

- Equation (10) is used again for the new roughness length, here $z_{0,r} = 0.05$ m, to obtain new frictional velocity $u_{*,r}$ and again, with $z_{0,r}$ and $u_{*,r}$, Equation (9) gives u_{st}.

The winds at 50 m are used for the generalization using the correction factors at the corresponding height. Only land area is handled so far.

6 Results

There are three parts in the application of the method, namely, the identification of storms, the mesoscale modeling and the post-processing.

The current study selects two areas for the production of the mesoscale extreme wind atlases, Denmark and the Gulf of Suez. This is to test the feasibility of the methodology for various extreme wind conditions, in terms of mechanisms and scales. For the Gulf of Suez where we expect that the mesoscale channeling winds contribute mainly to the extreme wind. There is a chance that these strong wind events will not be identified by the coarse resolution NCEP/NCAR reanalysis data. This is however not the case here owning to that the strongest channeling winds are in connection with the synoptical pressure distribution over the area. For the Denmark case, 100% of the extreme storms identified from measurements from a number of stations distributed all over Denmark are captured by the NCEP/NCAR reanalysis data and for the Gulf of Suez case 80% of the events identified from three stations are captured by the reanalysis data. The missed annual strongest wind cases are filled in by using the second or third strongest event, which gives a difference between 0.5 to 2 m/s in the 10-min wind speeds in this study.

When applying the post-processing approach-I, the annual wind maxima from each mesoscale model grid point are used with AMM to obtain the 50-year wind at several heights. Because we will use the surface layer logarithmic law we choose the 50-year wind at 10 m for the generalization. The contour map for the 50-year wind at 10 m for domain III without post-processing is shown in Figure 4 and that for the 50-year standard wind, i.e. at 10 m over a roughness length of 0.05 m, is shown in Figure 5. Note, for the water grid points, in order to make a smooth transition of the standard extreme wind from water to land, we estimate the roughness length by using the Charnock formula $z_0 = \alpha_{ch} u_*^2 / g$, with the Charnock parameter $\alpha_{ch} = 0.05$. The results are satisfactory except for

some grid points along the coastline, where apparently the effect of roughness is overestimated. Also in places representing cities and towns where the WRF roughness length is much higher than those for the surrounding grid points (here the roughness length of 0.5 m), the wind generalization produces hot spots as shown in Figure 5.

When applying the post-processing approach-II, we first correct the effect of orography, roughness change and the roughness for the simulated winds from each storm episode according to the direction and then use AMM to obtain the 50-year standard wind. The result is shown in Figure 6.

In Table 2 and Table 3 we list the estimation of the 50-year wind from measurements and simulation. For several sites, the locations are not amidst a homogeneous land or water surface, therefore a comparison based on the winds at the measuring height without post-processing in Table 2 is often inaccurate. Nevertheless, the agreement between the 50-year wind from measurements and simulation is rather good. The agreement is indeed improved after using the post-processing approach-I while the values from the post-processing approach-II are considerably smaller due mostly to the smoothed effective roughness length obtained from LINCOM (Table 3).

The main data validation has so far been done to the Denmark case. For the Gulf of Suez, there shows a very good agreement between the measured and simulated extreme wind characteristics, reflected in the directional annual wind maxima distribution at several sites along the Gulf. For two of the sites where the measurements are longer than 7 years, the 50-year winds (without post-processing) from the simulation (2000-2009) are 23.1 and 23.6 m/s at a height of 24.5 m, and the corresponding numbers from the measurements (1991-2005) are 23.7 ± 3.6 and 25.4 ± 3.8 m/s.

7   Discussions

The generalized extreme winds from the WRF simulations through the post-processing provide mesoscale background wind force and they can be applied to specific sites through microscale modeling, e.g. WEng.
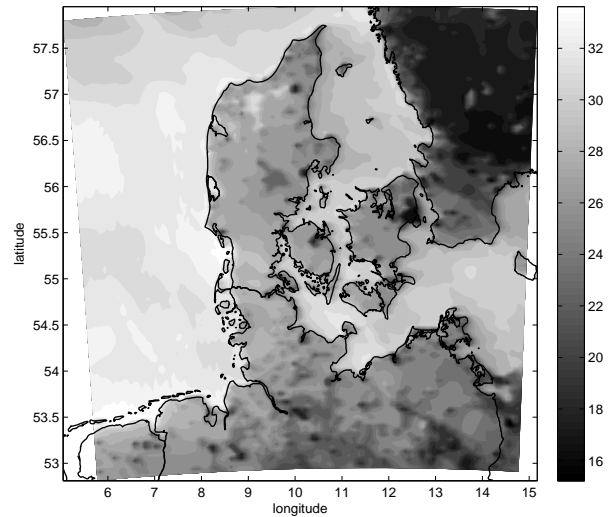

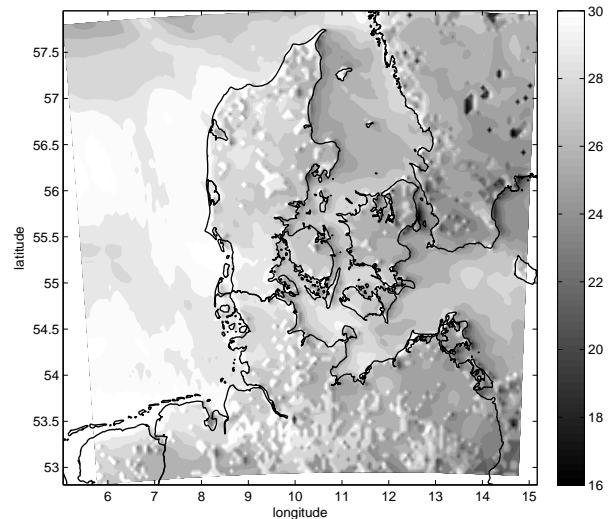Figure 4: The 50-year wind at 10 m, domain III, without post-processing.

Figure 5: The 50-year standard wind, here at 10 m, over roughness length of 0.05 m, using post-processing approach-I, domain III.

Table 2: The 50-year wind at measuring height, observed and simulated

Stations	Height (m)	U_{50} (m/s) WRF	$U_{50} \pm 1.96\sigma$ (m/s) OBS
Sprogø	70	35.7	33.0 ± 3.7
Tystofte	39	32.4	31.5 ± 4.5
Kegnæs	23.4	31.7	35.8 ± 7.0
Jylex	24	33.8	35.4 ± 5.5
Risø	76.6	32.9	33.2 ± 5.4
Horns Rev	62	41.2	44.2 ± 14.0
FINO1	50	39.3	38.1 ± 8.8

Table 3: The 50-year standard wind, i.e. at 10 m, over roughness of 0.05 m, from measurement ($\pm 1.96\sigma$) and simulation. WRF 1 and 2 refer to that the post-processing approach-I and II are used, respectively. "*": values from [2]; "-": not provided.

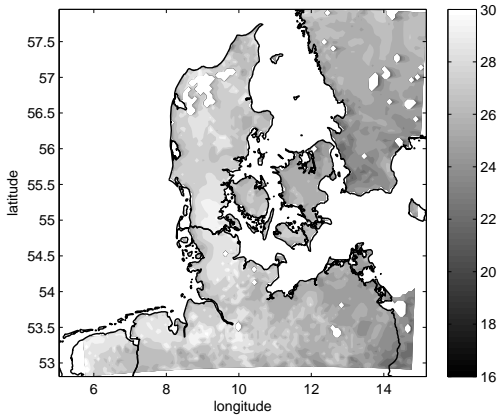| Stations	WRF 1	WRF 2	OBS
Sprogø	24.7	21.1	23.9 ± 2.0 *
Tystofte	26.1	25.1	25.7 ± 2.9 *
Kegnæs	26.0	22.4	26.3 ± 3.8 *
Jylex	30.2	25.0	29.1 ± 2.9 *
Horns Rev	30.1	-	31.6 ± 8.5
FINO1	29.7	-	30.3 ± 7.6

Figure 6: The 50-year standard wind, here at 10 m, over roughness length of 0.05 m, using post-processing approach-II, domain III, over land only.

In the first of the three steps of the selective dynamical downscaling method, i.e. identification of extreme wind events, we have used the ~ 200 km resolution NCEP/NCAR reanalysis data. It is economical and turns out to be successful for both cases here, due to the fact that the extreme wind events are related to synoptic scale weather phenomena. However, we would expect less satisfactory results for places where these events are rather local. For such situations, reanalysis data that are of finer spatial and/or temporal resolutions (e.g. MERRA and CFSR) are expected to improve the method.

Each individual storm was validated by comparing the meteorological parameters such as wind speed, direction, temperature and pressure from the simulations with the measurements available at all sites. Both measured and simulated extreme winds are affected by the uncertainty induced by data length and long term variability in the extreme wind. Therefore, a stationary extreme wind climate is assumed. The general agreement between the extreme winds estimation from measurement and simulation is very good.

The simple version of post-processing

approach-I seems to provide satisfactory results at the measurements sites, while the more sophisticated approach-II seem to underestimate the standard winds. It was found that the effects due to changes in topography and upstream roughness are rather small compared to that from the effective roughness length. The effective roughness length was derived from the linear model LINCOM based on the roughness map from WRF. Compared to the aerodynamic roughness length used in WRF, the effective roughness is on average of smaller values, leading to the generalized winds of smaller values in general. This could be a result of the fact that the roughness effects in LINCOM and in the WRF simulation are not consistently handled. More work needs to be done to bridge this difference.

8 Conclusions

The selective dynamical downscaling method is an efficient tool which set its focus on the most important factors in extreme wind estimation, namely the most severe storms. The extreme wind atlases seem promising, as validated by measurements from several sites. The post-processing approach-II, which seem to suffer from the inconsistency between LINCOM and WRF in treating the roughness effect, and further research is needed here.

References

[1] Eurocode. Eurocode 1, basis of design and actions on structure – Parts 2 – 4: actions on structure – wind actions. Technical report, European committee for standardization, Rue de Stassart, Brussels, 1995.

[2] X.G. Larsén and J. Mann. Extreme winds from the NCEP/NCAR reanalysis data. *Wind Energy, DOI: 10.1002/we.318*, 12:556–573, 2009.

[3] M.G. Sotillo. A high-resolution 44-year atmospheric hindcast for the Mediterranean Basin: Contribution to the regional improvement of global reanalysis. *Climate Dynamics, DOI 10.1007/s00382-005-0030-7*, 25:219–236, 2005.

[4] X.G. Larsén, J. Mann, H. Göttel, and D. Jacob. Wind climate and extreme winds from the regional climate model REMO. In: Scientific Proceedings (on line). European Wind Energy Conference and Exhibition, Brussels, 31 March - 3 April, pages 58–62. 2008.

[5] J. Badger, X. G. Larsén, N.G. Mortensen, A. Hahmann, J.C. Hensen, and H. Jørgensen. A universal mesoscale to microscale modelling interface tool. European Wind Energy Conference, Warsaw, Poland, 20 - 23 April, 6 pages. 2010.

[6] J. Abild. Application of the wind atlas method to extremes of wind climatology. Technical Report Risoe-R-722(EN), Risø National Laboratory, Roskilde, Denmark, 1994.

[7] J. Mann, L. Kristensen, and N. O. Jensen. Uncertainties of extreme winds, spectra and coherences. In Larsen and Esdahl, editors, *Bridge Aerodynamics, ISBN 9054109610*. Rotterdam, Balkema, 1998.

[8] L. Kristensen, O. Rathmann, and S. O. Hansen. Extreme winds in Denmark. *J. Wind Eng. Ind. Aerodyn.*, 87:147–166, 2000.

[9] H. Tennekes. Similarity relations, scaling laws and spectral dynamics. In F. T. M. Nieuwstadt and H. van Dop, editors, *Atmospheric turbulence and air pollution modelling*, chapter 2, pages 37–68. D. Reidel publishing company, Dordrecht, 1982.

[10] L. Landberg, L. Myllerup, O. Rathmann, E.L. Petersen, B.H. Jørgensen, J. Badger, and N.G. Mortensen. Wind resource estimation - An overview. *Wind Energy*, 6:261–271, 2003.